Published in final edited form as:
Eur J Nucl Med Mol Imaging. 2009 May ; 36(5): 811–822. doi:10.1007/s00259-008-1039-z.

FDG-PET changes in brain glucose metabolism from normal cognition to pathologically verified Alzheimer's disease

Lisa Mosconi
Department of Psychiatry, New York University School of Medicine, New York, USA

Center for Brain Health, MHL 400, New York University School of Medicine, 560 First Avenue, New York, NY 10016, USA

Rachel Mistur and **Remigiusz Switalski**
Department of Psychiatry, New York University School of Medicine, New York, USA

Wai Hon Tsui
Department of Psychiatry, New York University School of Medicine, New York, USA

Nathan Kline Institute, Orangeburg, NY, USA

Lidia Glodzik, **Yi Li**, **Elizabeth Pirraglia**, **Susan De Santi**, and **Barry Reisberg**
Department of Psychiatry, New York University School of Medicine, New York, USA

Thomas Wisniewski
Department of Psychiatry, New York University School of Medicine, New York, USA

Department of Neurology, New York University School of Medicine, New York, USA

Department of Pathology, New York University School of Medicine, New York, USA

Mony J. de Leon
Department of Psychiatry, New York University School of Medicine, New York, USA

Nathan Kline Institute, Orangeburg, NY, USA

Abstract

Purpose—We report the first clinicopathological series of longitudinal FDG-PET scans in post-mortem (PM) verified cognitively normal elderly (NL) followed to the onset of Alzheimer's-type dementia (DAT), and in patients with mild DAT with progressive cognitive deterioration.

Methods—Four NL subjects and three patients with mild DAT received longitudinal clinical, neuropsychological and dynamic FDG-PET examinations with arterial input functions.NL subjects were followed for 13±5 years, received FDG-PET examinations over 7±2 years, and autopsy 6±3 years after the last FDG-PET. Two NL declined to mild cognitive impairment (MCI), and two developed probable DAT before death. DAT patients were followed for 9±3 years, received FDG-PET examinations over 3±2 years, and autopsy 7±1 years after the last FDG-PET. Two DAT patients progressed to moderate-to-severe dementia and one developed vascular dementia.

Results—The two NL subjects who declined to DAT received a PM diagnosis of definite AD. Their FDG-PET scans indicated a progression of deficits in the cerebral metabolic rate for glucose

e-mail: lisa.mosconi@med.nyu.edu.

Electronic supplementary material The online version of this article (doi:10.1007/s00259-008-1039-z) contains supplementary material, which is available to authorized users.

(CMRglc) from the hippocampus to the parietotemporal and posterior cingulate cortices. One DAT patient showed AD with diffuse Lewy body disease (LBD) at PM, and her last in vivo PET was indicative of possible LBD for the presence of occipital as well as parietotemporal hypometabolism.

Conclusion—Progressive CMRglc reductions on FDG-PET occur years in advance of clinical DAT symptoms in patients with pathologically verified disease. The FDG-PET profiles in life were consistent with the PM diagnosis.

Keywords

Dementia; Alzheimer's disease; FDG-PET; Positron emission tomography; Early detection

Introduction

The development of sensitive markers for the preclinical detection of neurodegenerative diseases such as Alzheimer's disease (AD) is a vital step in developing preventive measures. Testing a candidate marker for AD requires longitudinal monitoring of normal healthy elderly until they express the clinical symptoms and receive the ultimate diagnostic confirmation post mortem. Currently, only post-mortem examinations can demonstrate whether a patient with a clinical diagnosis of Alzheimer's-type dementia (DAT) really suffered from AD pathology or another neurodegenerative disease [1,2]. The definitive diagnosis of AD requires the presence of amyloid deposits and neurofibrillary tangles (NFT) in the hippocampus (HIP) and neocortex, which are typically associated with neuronal loss and volume reductions [1,3].

Positron emission tomography (PET) imaging with 2-[^{18}F] fluoro-2-deoxy-$_{D}$-glucose (FDG) is a candidate modality for detecting the preclinical stages of AD by measuring reductions in the cerebral metabolic rate for glucose (CMRglc). FDG-PET studies have shown that CMRglc is consistently reduced in patients with DAT, particularly in the parietotemporal, posterior cingulate (PCC), and medial temporal and/or frontal cortices, the extent of the CMRglc reductions being related to disease severity (see reference [4] for review). Reduced CMRglc predicts the onset of DAT in patients with mild cognitive impairment (MCI) [5-7]. Moreover, recent FDG-PET studies have shown that CMRglc reductions in the hippocampal formation, a known early target for AD pathology [8], predict the transition from normal cognition to MCI and dementia, and correlate with clinical progression [9,10].

Although these FDG-PET studies have shown clinical correlates of CMRglc reductions, there are no studies validating these longitudinal observations with neuropathological data. Neuropathological confirmation of the clinical diagnosis associated with the progression of CMRglc abnormalities is essential to validate in vivo FDG-PET measures as predictors and correlates of prodromal AD.

We present here four normal individuals followed longitudinally for 13±5 years (range 9-19 years) to the onset of clinical symptoms of MCI and DAT with clinical, neuropsychological and parallel FDG-PET examinations, and to the post-mortem confirmation of AD diagnosis. We contrast them with three DAT patients followed for 9±3 years (range 7-12 years) with classical initial memory dysfunction and pathologically proven AD.

Materials and methods

Subject screening and diagnostic examinations

Seven subjects presented to the Center for Brain Health at the New York University (NYU) School of Medicine between 1980 and 1992 and were followed longitudinally until their demise at which time they received post-mortem examinations. All subjects were community-residing

volunteers participating in ongoing studies of normal aging and dementia. Subjects received extensive baseline evaluations that were repeated at each successive follow-up, which included medical, neurological, and neuropsychological examinations, blood analysis, and clinical brain MRI. The ApoE genotype was determined using standard polymerase chain reaction [9]. The psychometric battery included the mini mental state examination (MMSE), immediate and delayed recall of a paragraph and of paired associates, the designs, the digitsymbol substitution (DSST), visual recognition, and the object-naming tests [9-11]. The global deterioration scale (GDS) was used to define patients as having MCI (GDS 3), mild (GDS 4), moderate (GDS 5-6) or severe (GDS 7) dementia in life and at the time of death [12].

All subjects received at least two FDG-PET scans within 2 months of the clinical examinations. For four subjects, the baseline clinical evaluations corresponded to the first FDG-PET examination, and the remaining three subjects received clinical examinations also before the first PET scan, as specified in each report and shown in Supplementary File 1. Informed consent was obtained from all subjects, and from a caregiver for patients diagnosed with dementia. The study was approved by the NYU and Brookhaven National Laboratory (BNL, Upton, NY) IRB.

Categorization into diagnostic groups represented a clinical judgment made at a consensus meeting. Conditions affecting brain structure or function (e.g., stroke, clinically uncontrolled diabetes, significant head trauma, active evidence of depression), or use of medications which adversely affect cognition, led to exclusion at baseline and at follow-up. None of the subjects had a modified Hachinski ischemia score of >4 [13]. Four subjects were diagnosed as clinically and cognitively normal (NL) at baseline, with a MMSE score of ≥28 and a GDS score of ≤2 [12]. Three subjects had a baseline diagnosis of DAT according to the NINCDS-ADRDA [3] and the DSM-IV [14] criteria, and had a GDS score of 4 [12], indicating dementia of mild severity.

At each follow-up, subjects were re-examined at the consensus meeting for a change in clinical diagnosis and disease worsening. The diagnosis of MCI was based on a clinician interview reporting evidence of reduced cognitive capacity from a prior level of functioning, but with normal activities of daily living and no dementia [3,13,14], and on a testimony from a knowledgeable collateral source, resulting in a GDS score of 3 [12]. Fixed cut-off scores on neuropsychological testing were not used for the clinical diagnosis of MCI. Each subject's psychometric scores were retrospectively *Z*-scored relative to a normal control group [15] to classify MCI patients as `amnestic' (memory scores >1.5 SD below norms) and `non-amnestic' [16].

Post-mortem examinations

At the time of autopsy, the brain was weighed, and the brainstem and attached cerebellum were separated from the cerebral hemispheres by a horizontal incision at the diencephalomesencephalic junction. The left cerebral hemisphere, the attached half of the midbrain, and the hemi-brainstem and cerebellum were immersion-fixed in 10% buffered formalin. The right cerebral hemispheres were cut coronally and frozen. Following fixation, the left hemispheres were cut coronally into 5-mm thick slabs and 16 standard regions were sampled, paraffin-embedded and sectioned. Sections from each block were examined with a Luxol Fast blue/hematoxylin and eosin combination stain, a Bielschowsky silver and a Congo red stain. Selected blocks were subjected to immunohistochemical staining using antibodies against abnormally phosphorylated tau, amyloid-β, α-synuclein and ubiquitin [17]. The Aβ and NFT burdens were assessed semiquantitatively following the Consortium to Establish a Registry of Alzheimer's Disease (CERAD) [1] and Braak and Braak staging [18] criteria, using the NIA-Reagan Institute criteria for the diagnosis of AD [19]. Autopsies were performed between 2000 and 2003 by the same neuropathologist (T.W.).

FDG-PET

All subjects received a PET scan at BNL using FDG as the tracer on an ECAT CTI-931 scanner (Siemens, Knoxville, TN) (axial FOV 10 cm, transaxial FOV 20 cm, in-plane axial resolution 6.2 mm, cross-slice FWHM 6.7 mm, interslice distance 6.75 mm). The subject's head was positioned using two orthogonal laser beams and imaged with the scanner tilted 25° negative to the canthomeatal plane. Subjects received 5-8 mCi of FDG intravenously while lying supine in a dimly lit room. PET images were obtained 35 min after injection and acquired over 20 min. Arterial blood samples were drawn at standard intervals throughout the study and CMRglc (μmol/100 g per minute) was calculated using Sokoloff's model with standard kinetic constants [20,21]. We obtained and interleaved two 15-slice PET volumes that overlapped by a half-slice thickness (about 3.4 mm) to improve the counting statistics [9]. Data were reconstructed using filtered back-projection (Fourier rebinning/2-D back-projection, Hanning filter with a frequency cut-off of 0.5 cycles/pixel) and corrected for attenuation using $^{68}Ga/^{68}Ge$ transmission scans, scatter and radioactive decay, yielding a 128×128 matrix with a pixel size of 1.56 mm.

MRI

All subjects received a standardized whole-brain MRI scan protocol, including a clinical and a research scan. Two 1.5-T magnets were used, a Philips Gyroscan (Philips International, Eindhoven, The Netherlands) and a G.E. Advantage (General Electrics, Milwaukee, WI). The diagnostic study was a contiguous 3-mm axial T2-weighted image. The research scan was a 3-D T1-weighted image, acquired either with a spin-echo sequence (Philips; TR 630 ms, TE 20 ms, matrix 204×256, FOV 23 cm) or a fast-gradient-echo sequence (Signa; TR 35 ms, TE 9 ms, matrix 256×128, FOV 25 cm). These scans were used to rule out MRI evidence of hydrocephalus, intracranial mass, strokes, subcortical gray matter lacunes, moderate to severe non-specific white matter disease, and focal white matter hyperintensities [22].

Image analysis

FDG-PET analysis was performed using the Neurological Statistical Image Analysis package (NEUROSTAT; University of Seattle, WA) [23]. Each FDG-PET scan was subjected to rotational correction and centering in three dimensions, followed by realignment to the anterior-posterior commissure line, and warping to the common stereotactic coordinate system of Talairach and Tournoux [24] using a 12-parameter affine transformation followed by nonlinear warping. The spatially normalized FDG-PET scans of each subject were compared with a reference normal database generated from the FDG-PET scans of 55 longitudinally followed NL individuals [25]. The FDG-PET scans of the database were acquired using the same PET scanner and procedures as with the subjects included in this study. Each FDG-PET scan of the seven patients under study was compared with the database after controlling for the global CMRglc, and Z scores [$Z = (\text{mean}_{\text{subject}} - \text{mean}_{\text{database}})/\text{SD}_{\text{database}}$] were calculated on a voxel-wise basis at $p \leq 0.05$ (one-tailed) [23,25]. Gray matter activities were extracted to predefined surface pixels using a three-dimensional stereotactic surface projection technique (3D-SSP) to examine on an individual basis the extent, topography and progression of CMRglc reductions [23].

Automated regions of interest (ROI) were used to sample CMRglc from the spatially normalized PET within specific AD-related brain regions (HIP, inferior parietal lobe, lateral temporal lobe, PCC, and prefrontal cortex) [10,26,27].

Statistical analysis

Statistical analyses were done using SPSS 12.0 (SPSS, Chicago, IL). Descriptive statistics included the arithmetic mean, median, and standard deviation (SD). The nonparametric

Spearman's rho (ρ) correlation test (α=0.05, one-tailed, exact inference) was used to examine the relationship between ROI CMRglc at the last PET examination, dementia severity before death, and Braak staging of AD pathology across all subjects.

Results

Subjects' characteristics are summarized in Table 1. Of the four baseline NL subjects, two received a last clinical diagnosis of MCI, and two went through an MCI stage and then declined to DAT. Of the three baseline DAT patients, one was subsequently diagnosed with vascular dementia and the remaining two retained a diagnosis of DAT.

Baseline normal subjects

Patient 1—This patient was clinically followed for 19 years (1980-1999), and received four FDG-PET examinations (1991, 1993, 1996, and 1999). He was married, had a Masters degree and was a retired manager. He had brother with a diagnosis of late-onset DAT and pathologically confirmed AD. At the first clinical examination in 1980, the subject was 70 years old, clinically and cognitively NL, with MMSE score 29 and GDS score 2. At the time of the first FDG-PET, the subject was 81 years old, still clinically and cognitively NL, with MMSE score 29 and GDS score 2. He had declined to MCI in 1994, shortly after his second PET scan. At this point, he was complaining of decreased concentration ability and gaps in recent memory, and developed attention deficits. During subsequent evaluations, the patient became less organized, reported becoming more cautious in performing complex motor tasks, especially driving, and more forgetful.

As shown in Fig. 1, no CMRglc abnormalities were found on the first FDG-PET scan in 1991. At the time of the first follow-up FDG-PET scan, when the subject was still clinically normal, significant hypometabolism was observed in the HIP, while the cortical regions did not show significant abnormalities. The same abnormalities were found on the second follow-up FDG-PET scan after the diagnosis of MCI. The last FDG-PET scan in 1999 showed hypometabolism in the HIP, and in the PCC and temporal cortices of the left hemisphere (Fig. 1).

The patient died at age 91 years, 1 year after the last clinical examination, of acute myocardial infarction. Neuropathological examination after death demonstrated AD-related pathology (CERAD possible, Braak and Braak stage IV).

Patient 2—This subject was followed for 14 years (1980-1994), and received two FDG-PET examinations in 1989 and 1994. He was originally from Argentina, but had lived most of his life in the United States. He was married, had finished college and was a retired manager. At the first clinical examination, the subject was 71 years old, clinically and cognitively normal, with MMSE score 30 and GDS score 2. At the time of the first FDG-PET, he was 80 years old, and still normal (MMSE score 30, GDS score 2). The subject's chief complaint was a lack of motivation, besides forgetting names, times and locations. All neuropsychological tests were within norms. In 1994, at the time of his second FDG-PET scan, the patient received a diagnosis of MCI and showed a slowing of gait and movement and overt word finding difficulties. Cognitive deficits were restricted to delayed recall tests with scores >1.5 SD below norms, which retrospectively describe the patient as an amnestic MCI [16].

The progression of CMRglc deficits in this subject is shown in Fig. 2. The baseline FDG-PET scan showed moderate HIP hypometabolism in the absence of cortical abnormalities (Fig. 2a). The follow-up FDG-PET scan, which corresponded to an MCI diagnosis, showed more reduced CMRglc in the HIP, bilaterally, and in the right PCC and anterior cingulate cortex, and a trend towards reduced right temporal CMRglc, which did not reach statistical significance (Fig. 2).

The patient died in 2002 at age 93 years, 8 years after the last clinical and FDG-PET examinations. Post-mortem examination led to a primary neuropathological diagnosis of Parkinson's disease with Lewy bodies in the substantia nigra, with mild AD-related pathology (CERAD possible, Braak and Braak stage III), and moderate congophilic angiopathy.

Patient 3—This subject was clinically followed for 9 years (1988-1997), and received four FDG-PET examinations (1989, 1992, 1996, and 1998). At the first visit, she was 69 years old, clinically and cognitively normal, with MMSE score 30 and GDS score 2. She was married, had finished high school, and was a retired stenographer. She had a twin with a diagnosis of late-onset DAT and pathologically confirmed AD. Neuropsychological measures were within the normal range during clinical visits from 1988 to 1993. She was diagnosed with MCI in 1996. The subject received MMSE score 28 and showed a decline in verbal memory scores. She had declined to DAT (mild dementia, GDS score 4 and MMSE score 25) in 1997.

The progression of CMRglc deficits in this subject is shown in Fig. 3. On both baseline and first follow-up FDGPET scans, when the subject was still clinically normal, CMRglc reductions were restricted to the HIP (Fig. 3a). The second follow-up FDG-PET scan showed CMRglc reductions in the HIP, temporal, and to a lesser extent, parietal cortices, bilaterally. The last FDG-PET scan, at which time the patient had developed DAT, showed a more extended topography of cortical CMRglc reductions in the parietotemporal, frontal and anterior cingulate regions, bilaterally (Fig. 3b). The parietotemporal CMRglc reductions were more pronounced in the right hemisphere. The PCC was not hypometabolic. Overall, the patient showed evidence of parietotemporal hypometabolism consistent with AD, and additional frontal hypometabolism.

The patient died of acute myocardial infarction in 2004 at age 85 years, 6 years after the last FDG-PET examination. Neuropathological examination demonstrated definite AD (CERAD definite, Braak stage VI) with additional mild subcortical leukoencephalopathy.

Patient 4—This subject received clinical examinations over 10 years (1992-2002), and received three FDG-PET examinations (1992, 1994, and 1997). At baseline, she was 69 years old, clinically and cognitively normal, with MMSE score 29 and GDS score 2. She was married, had finished high school, and was still working as a bookkeeper. Significant family history included mother's death at 90 years with a diagnosis of DAT and father's severe cardiovascular disease resulting in death at age 56 of a myocardial infarct. At the second follow-up in 1994, the subject received a diagnosis of MCI [12] with MMSE score 24. She exhibited isolated memory deficits $\geq$2 SD below norms, which in retrospect is consistent with amnestic MCI [16]. She had declined to moderate DAT (GDS score 5, MMSE score 23) in 1996. At her final clinical evaluation in 2002, the patient retained the diagnosis of DAT (GDS score 7).

The progression of CMRglc deficits in this subject is shown in Fig. 4. The baseline FDG-PET scan showed HIP hypometabolism in the absence of significant cortical abnormalities (Fig. 4a). The first follow-up FDG-PET scan, when the patient was diagnosed as MCI, showed more severe CMRglc reductions in the HIP, PCC and parietotemporal cortices, bilaterally, which had become more extended at the last follow-up FDG-PET (Fig. 4b, c). This FDG-PET pattern is consistent with a neurodegenerative disease such as AD.

The patient died of cardiac complications in 2003 at age 81 years, 6 years after the last FDG-PET examination. Neuropathological examination demonstrated definite AD (CERAD definite, Braak stage VI) with additional diagnoses of mild Lewy body disease (LBD), moderate hypertensive vascular changes and congophilic angiopathy.

Baseline DAT subjects

Patient 5—This subject received clinical examinations over 12 years (1987-1999), and two FDG-PET examinations, in 1990 and 1995. At the first clinical examination, she was 64 years old and was diagnosed with mild DAT with GDS score 4 and MMSE score 18. She was married, had finished college, and was a housewife. The patient's medical history included a mother with DAT. Additional clinical findings included a right bundle branch block and hypertension. At the time of the first FDG-PET scan, she received GDS score 6 and MMSE score 11, and showed severe memory deficits. At the time of the last clinical examination, she received a clinical diagnosis of severe DAT with GDS score 7 and MMSE score 0, and was not able to complete any of the neuropsychological tests.

As shown in Fig. 5, at both time points, FDG-PET examinations showed severe CMRglc reductions in the HIP, PCC and parietotemporal cortex, bilaterally, and in the right occipital cortex. Cortical hypometabolism was more pronounced in the right than in the left hemisphere (Fig. 5b). The subject showed FDG-PET evidence of a neurodegenerative disease consistent with AD with additional occipital hypometabolism, which is a well-established feature of LBD [28]. Frontal hypometabolism was evident on the baseline PET scan but not on follow-up.

The patient died in 2001 at age 77 years, 6 years after the last FDG-PET examination. Neuropathological examination demonstrated definite AD (CERAD definite, Braak stage V) with additional diagnoses of diffuse LBD, and moderate congophilic angiopathy.

Patient 6—This subject received clinical examinations over 7 years (1991-1998), and two FDG-PET examinations, in 1991 and 1993. At the time of the first visit, she was 69 years old, and was diagnosed with mild DAT with GDS score 4 and MMSE score 27. She was married, had finished high school, and was a retired manager. She showed severe memory and attention deficits, which had worsened at follow-up. At the patient's last clinical follow-up, she was diagnosed with probable vascular dementia, signifying a significant cerebrovascular component superimposed upon the AD profile. She received GDS score 6 and MMSE score 1, and was not able to complete any of the neuropsychological tests apart from the DSST.

The progression of CMRglc deficits on FDG-PET scans is shown in Fig. 6. The baseline FDG-PET scan showed CMRglc reductions in the HIP, bilaterally, and in the parietotemporal regions in the left hemisphere. Progressive CMRglc reductions within the same regions were observed on the follow-up FDG-PET scan in 1993. The PCC did not appear as hypometabolic.

The patient died in 2000 at age 79 years, 7 years after the last FDG-PET examination. Neuropathological examination after death demonstrated definite AD (CERAD definite, Braak stage VI) with moderate congophilic angiopathy and mild subcortical leukoencephalopathy.

Patient 7—This subject was followed clinically for 7 years (1992-1999), with two FDG-PET examinations in 1993 and 1995. At baseline, he was 77 years old and was diagnosed with mild DAT with GDS score 4 and MMSE score 27. He was married, had finished high school, had formerly worked in the media industry, and was retired. At the second clinical follow-up in 1996, he retained the diagnosis of DAT, with GDS score 5 and MMSE score 20.

The FDG-PET scans of this patient are shown in Fig. 7. The baseline FDG-PET scan showed CMRglc reductions in the HIP and in the parietal regions, and to a lesser extent in the PCC and temporal cortex of the left hemisphere. More severe CMRglc reductions within the same regions were observed on the follow-up FDG-PET scan in 1995 (Fig. 7b), with the left hemisphere showing more severe hypometabolism than the right.

The patient died of pneumonia in 2000 at age 84 years, 5 years after the last FDG-PET examination. Neuropathological examination after death demonstrated definite AD (CERAD definite, Braak stage V) with moderate congophilic angiopathy and mild subcortical leukoencephalopathy.

Correlating CMRglc with dementia severity and Braak stages

Dementia severity in life (i.e., last GDS score) correlated with CMRglc at the last FDG-PET examination in the left HIP (ρ=-0.64, $p \leq 0.05$) and in the PCC (ρ=-0.71, $p \leq 0.05$), and showed a trend in the left parietal cortex (ρ=-0.42, p=0.093). Braak staging of NFT pathology correlated with CMRglc at the last FDG-PET examination in the PCC (ρ=-0.65, $p \leq 0.05$), frontal (ρ=-0.66, $p \leq 0.05$), and parietal cortices (ρ=-0.58, $p \leq 0.05$), and there was a trend for the HIP (ρ=-0.50, p=0.091). There were no significant correlations between Braak stage and dementia severity at the last clinical examination before death ($p > 0.1$, n.s.).

Discussion

This FDG-PET study tracked the progression of CMRglc abnormalities during the decline from normal cognition to the onset of clinical symptoms of MCI and DAT, with postmortem verification of diagnosis. Longitudinal FDG-PET examinations in this cohort demonstrated that CMRglc reductions precede the onset of clinical symptoms by many years and correlate with dementia severity in life and pathological diagnosis of AD. Furthermore, the present results offer temporal and topographical in vivo information on the progressive involvement of different brain regions in the development of AD. Although FDG-PET profiles somewhat varied across subjects, CMRglc reductions were consistently detected in the HIP (Supplementary File 2), followed by the parietotemporal and PCC cortices at the MCI or mild dementia stages. HIP CMRglc reductions appeared to precede those in the cortical regions in cognitively normal individuals declining to DAT, while the cortical hypometabolism became evident by the time of the expression of symptoms.

The regional progression of the CMRglc abnormalities foreshadowing the onset of AD had not been clearly defined because of the lack of longitudinal FDG-PET studies with post-mortem verification. Previous FDG-PET studies that explored the preclinical stages of AD relied on the clinical diagnosis as the gold standard against which imaging measurements were compared because of the lack of post-mortem data. The few PET studies that followed cognitively normal individuals over time showed that CMRglc reductions in the hippocampal formation predict future cognitive decline and are longitudinally associated with the progression to MCI and late-onset AD in sporadic cases [9,10]. These studies also provided evidence for a progression of CMRglc reductions originating in the HIP and extending to the PCC and temporal cortices prior to the involvement of other neocortical regions during the decline from normal cognition to DAT [10].

The present FDG-PET findings substantiate prior longitudinal observations without post-mortem examinations by showing a progression of CMRglc deficits from the HIP to the association cortices in pathologically confirmed normal individuals who developed MCI and DAT, and in patients with mild DAT who further deteriorated over time. These in vivo imaging findings are consistent with the idea of progressive pathological spreading in AD from the hippocampal formation to the association cortex [8] and with the Braak and Braak staging model of NFT pathology in AD [18]. Studies have shown that the progression of NFT in the brain can be staged and that the pathological changes develop many years before the clinical manifestations of the disease become apparent using standard approaches to assessment [18, 29,30]. The pattern of hypometabolism seen in the progression of individuals from normal aging to AD is consistent with Braak stages of NFT pathology determined at autopsy.

Moreover, CMRglc in AD-related regions correlated with Braak stages of NFTs and with dementia severity in life.

Our findings are in agreement with previous observations of a relationship between CMRglc and CBF reductions in AD and regional densities of NFTs [31,32]. These cross-sectional findings did not provide direct evidence for longitudinal progression of brain abnormalities, which could only be inferred from contrasting groups of individuals at different stages of NFT pathology. Our longitudinal FDG-PET studies allowed direct examination of the temporal and topographical progression of disease.

Our findings showed a good correspondence between FDG-PET findings in life and histopathological diagnosis. The two patients who declined from NL to DAT and received a post-mortem diagnosis of definite AD (patients 3 and 4) already showed a clear FDG-PET pattern of hypometabolism in the parietotemporal, PCC and medial temporal cortices at the MCI stage. On the other hand, the two patients who declined from NL to MCI but did not progress to DAT or show definite post-mortem evidence of AD pathology (patients 1 and 2) did not present with FDGPET evidence for AD in life. For example, patient 2 presented with apathy and forgetfulness at the first examination, and developed memory deficits and motor difficulties at follow-up. This patient showed mild CMRglc reductions in life, involving the HIP and cingulate cortices, and LBD pathology at death with AD-related features, mainly NFT in the limbic lobes (Braak stage III). These data suggest that the patient's symptoms in life may have been related to an interaction between different disease processes, with NFT pathology possibly accounting for hypometabolism in memory-related regions and amnestic symptoms, and LBD pathology for the motor symptoms.

FDG-PET examinations also appeared to be of value in detecting pathological features that were not clinically evident. For example, patient 5 retained a clinical diagnosis of DAT throughout the study period and showed pathological features of AD and additionally diffuse LBD. The FDG-PET scan showed parietotemporal with additional occipital hypometabolism, which is a well-established feature of LBD [28]. FDG-PET in this patient reflected the presence of LBD pathology that was not detectable on clinical examination. Additionally, frontal hypometabolism was evident on the baseline PET but not at follow-up, suggesting that the frontal deficits in this patient were due to a reversible functional abnormality, whereas the HIP, PCC, parietotemporal and occipital hypometabolism was due to AD and LBD pathology.

In the largest FDG-PET series of patients with pathologically verified dementia available to date, the presence of CMRglc abnormalities on ante-mortem FDG-PET scan correctly predicted post-mortem AD diagnosis with 88% accuracy, including patients with mild dementia [33]. Our data indicate that CMRglc reductions consistent with AD can be detected prior to the onset of dementia and progress with dementia severity, suggesting that FDG-PET imaging has the potential for contributing to clinical diagnosis at the preclinical AD stages.

The present results are based on a limited number of patients and caution is required in the interpretation of the results, which need to be replicated with larger samples in order to test their generalizability to the population. Due to the small number of subjects, our analysis was based on the comparison of each PET scan to a database of healthy controls [25]. In view of using FDG-PET to develop preventive measures for AD, absolute quantitation of CMRglc is necessary. Additionally, we used two voxel-based analysis techniques, one that highlights hypometabolism in the form of 3D-SSP maps [23], and the other that enables quantification of CMRglc within specific ROIs [10,26]. We previously showed that whole-brain voxel-based analysis does not provide accurate quantification of CMRglc within small brain regions, such as the HIP, in AD [26]. Accordingly, in this study hippocampal hypometabolism was not

consistently detectable on the 3D-SSP images of the medial brain views, whereas it was significant using the anatomically precise ROI approach.

Our correlation analysis was based on descriptive statistics. We used a semiquantitative approach to characterize pathological lesions post mortem, and correlated Braak stages of NFT (range 0-6) with CMRglc. We could not examine correlations between amyloid load estimated using CERAD scores (i.e., possible or definite) and CMRglc, as five of the seven subjects were judged to have `definite' AD (Table 1). Quantitative histological studies are needed to directly examine the relationship between CMRglc, amyloid and NFT load. Lastly, we did not perform partial volume correction of the FDG-PET data because different MRI scanners were used throughout the years. Partial volume correction using MRI with different resolutions may hinder detection of longitudinal CMRglc changes. However, we have previously demonstrated that longitudinal CMRglc reductions observed in NL decliners to MCI/AD as compared to stable NL remain significant after partial volume correction, and therefore represent true reductions in CMRglc per gram of brain tissue [9,10].

Supplementary Material

Refer to Web version on PubMed Central for supplementary material.

Acknowledgments

This work was supported by the NIH-NIA grants AG12101, AG13616, AG08051, AG03051 and AG022374, NIH NCRR and MO1RR0096, and the Alzheimer's Association. We thank Joanna Fowler, David Schlyer and Gene-Jack Wang at BNL for their support of the PET studies, and Miroslaw Brys for his contribution to the paper.

References

1. Mirra SS, Heyman A, McKeel D, et al. Part II. Standardization of the neuropathologic assessment of Alzheimer's disease. Neurol 1991;41:479–86.
2. Price JL, Morris JC. Tangles and plaques in nondemented aging and “preclinical” Alzheimer's disease. Ann Neurol 1999;45:358–68. [PubMed: 10072051]
3. McKhann G, Drachman D, Folstein M, Katzman R, Price D, Stadlan EM. Clinical diagnosis of Alzheimer's disease: report of the NINCDS-ADRDA Work Group under the auspices of Department of Health and Human Services Task Force on Alzheimer's Disease. Neurology 1984;34:939–44. [PubMed: 6610841]
4. Mosconi L. Brain glucose metabolism in the early and specific diagnosis of Alzheimer's disease. Eur J Nucl Med 2005;32:486–510.
5. Chetelat G, Desgranges B, De La Sayette V, Viader F, Eustache F, Baron JC. Mild cognitive impairment: can FDG-PET predict who is to rapidly convert to Alzheimer's disease. Neurology 2003;60:1374–7. [PubMed: 12707450]
6. Drzezga A, Lautenschlager N, Siebner H, et al. Cerebral metabolic changes accompanying conversion of mild cognitive impairment into Alzheimer's disease: a PET follow-up study. Eur J Nucl Med Mol Imaging 2003;30:1104–13. [PubMed: 12764551]
7. Mosconi L, Perani D, Sorbi S, et al. MCI conversion to dementia and the APOE genotype: a prediction study with FDG-PET. Neurology 2004;63:2332–40. [PubMed: 15623696]
8. Ball MJ, Hachinski V, Fox A, et al. A new definition of Alzheimer's disease: a hippocampal dementia. Lancet 1985;1:14–6. [PubMed: 2856948]
9. de Leon MJ, Convit A, Wolf OT, et al. Prediction of cognitive decline in normal elderly subjects with 2-[18F]fluoro-2-deoxy-Dglucose/positron-emission tomography (FDG/PET). Proc Natl Acad Sci U S A 2001;98:10966–71. [PubMed: 11526211]
10. Mosconi L, De Santi S, Li J, et al. Hippocampal hypometabolism predicts cognitive decline from normal aging. Neurobiol Aging 2007;29:676–92. [PubMed: 17222480]

11. De Santi S, de Leon MJ, Rusinek H, et al. Hippocampal formation glucose metabolism and volume losses in MCI and AD. Neurobiol Aging 2001;22:529–39. [PubMed: 11445252]
12. Reisberg B, Ferris SH, de Leon MJ, Crook T. The global deterioration scale for assessment of primary degenerative dementia. Am J Psychiatry 1982;139:1136–9. [PubMed: 7114305]
13. Hachinski VC, Lassen NA, Marshall J. Multi-infarct dementia, a cause of mental deterioration in the elderly. Lancet 1974;2:207–10. [PubMed: 4135618]
14. Diagnostic and statistical manual of mental disorders. Vol. 4th ed.. American Psychiatric Association; Washington, D.C.: 1994.
15. De Santi S, Pirraglia E, Barr W, Babb J, Williams S, Rogers K, et al. Robust and conventional neuropsychological norms: diagnosis and prediction of age-related cognitive decline. Neuropsychology 2008;22:469–84. [PubMed: 18590359]
16. Petersen RC, Smith GE, Waring SC, Ivnik RJ, Tangalos EG, Kokmen E. Mild cognitive impairment: clinical characterization and outcome. Arch Neurol 1999;56:303–8. [PubMed: 10190820]
17. Wegiel J, Kuchna I, Nowicki K, et al. Intraneuronal Abeta immunoreactivity is not a predictor of brain amyloidosis-beta or neurofibrillary degeneration. Acta Neuropathol 2007;113:389–402. [PubMed: 17237937]
18. Braak H, Braak E. Neuropathological stageing of Alzheimerrelated changes. Acta Neuropathol 1991;82:239–59. [PubMed: 1759558]
19. Consensus recommendations for the postmortem diagnosis of Alzheimer's disease. Neurobiol Aging 1997;18:S1–2. [PubMed: 9330978]
20. Sokoloff L, Reivich M, Kennedy C, et al. The [14C]deoxyglucose method for the measurement of local cerebral glucose utilization: theory, procedure, and normal values in the conscious and anesthetized albino rat. J Neurochem 1977;28:897–916. [PubMed: 864466]
21. Reivich M, Alavi A, Wolf A, et al. Glucose metabolic rate kinetic model parameter determination in humans: the lumped constants and rate constants for [18F]fluorodeoxyglucose and [11C] deoxyglucose. J Cereb Blood Flow Metab 1985;5:179–92. [PubMed: 3988820]
22. George AE, de Leon MJ, Kalnin A, Rosner L, Goodgold A, Chase N. Leukoencephalopathy in normal and pathologic aging: 2. MRI and brain lucencies. AJNR Am J Neuroradiol 1986;7:567–70. [PubMed: 3088934]
23. Minoshima S, Giordani B, Berent S, Frey KA, Foster NL, Kuhl DE. Metabolic reduction in the posterior cingulate cortex in very early Alzheimer's disease. Ann Neurol 1997;42:85–94. [PubMed: 9225689]
24. Talairach, J.; Tournoux, P. Co-planar stereotaxic atlas of the human brain. Thieme; Stuttgart: 1988.
25. Mosconi L, Tsui WH, Pupi A, et al. (18)F-FDG PET database of longitudinally confirmed healthy elderly individuals improves detection of mild cognitive impairment and Alzheimer's disease. J Nucl Med 2007;48:1129–34. [PubMed: 17574982]
26. Mosconi L, Tsui WH, De Santi S, et al. Reduced hippocampal metabolism in mild cognitive impairment and Alzheimer's disease: automated FDG-PET image analysis. Neurology 2005;64:1860–7. [PubMed: 15955934]
27. Li Y, Rinne JO, Mosconi L, Pirraglia E, Rusinek H, Desanti S, et al. Regional analysis of FDG and PIB-PET images in normal aging, mild cognitive impairment and Alzheimer's disease. Eur J Nucl Med Mol Imaging 2008;35:2169–81. [PubMed: 18566819]
28. Minoshima S, Foster NL, Sima AA, Frey KA, Albin RL, Kuhl DE. Alzheimer's disease versus dementia with Lewy bodies: cerebral metabolic distinction with autopsy confirmation. Ann Neurol 2001;50:358–65. [PubMed: 11558792]
29. Braak H, Braak E. Development of Alzheimer-related neurofibrillary changes in the neocortex inversely recapitulates cortical myelogenesis. Acta Neuropathol 1996;92:197–201. [PubMed: 8841666]
30. Delacourte A, David JP, Sergeant N, et al. The biochemical pathway of neurofibrillary degeneration in aging and Alzheimer's disease. Neurol 1999;52:1158–65.
31. DeCarli C, Atack JR, Ball MJ, et al. Post-mortem regional neurofibrillary tangle densities but not senile plaque densities are related to regional cerebral metabolic rates for glucose life in Alzheimer's disease patients. Neurodegeneration 1992;1:113–21.

32. Bradley KM, O'Sullivan VT, Soper ND, et al. Cerebral perfusion SPET correlated with Braak pathological stage in Alzheimer's disease. Brain 2002;125:1772–81. [PubMed: 12135968]

33. Silverman DHS, Small GW, Chang CY, et al. Positron emission tomography in evaluation of dementia: regional brain metabolism and long-term outcome. JAMA 2001;286:2120–7. [PubMed: 11694153]

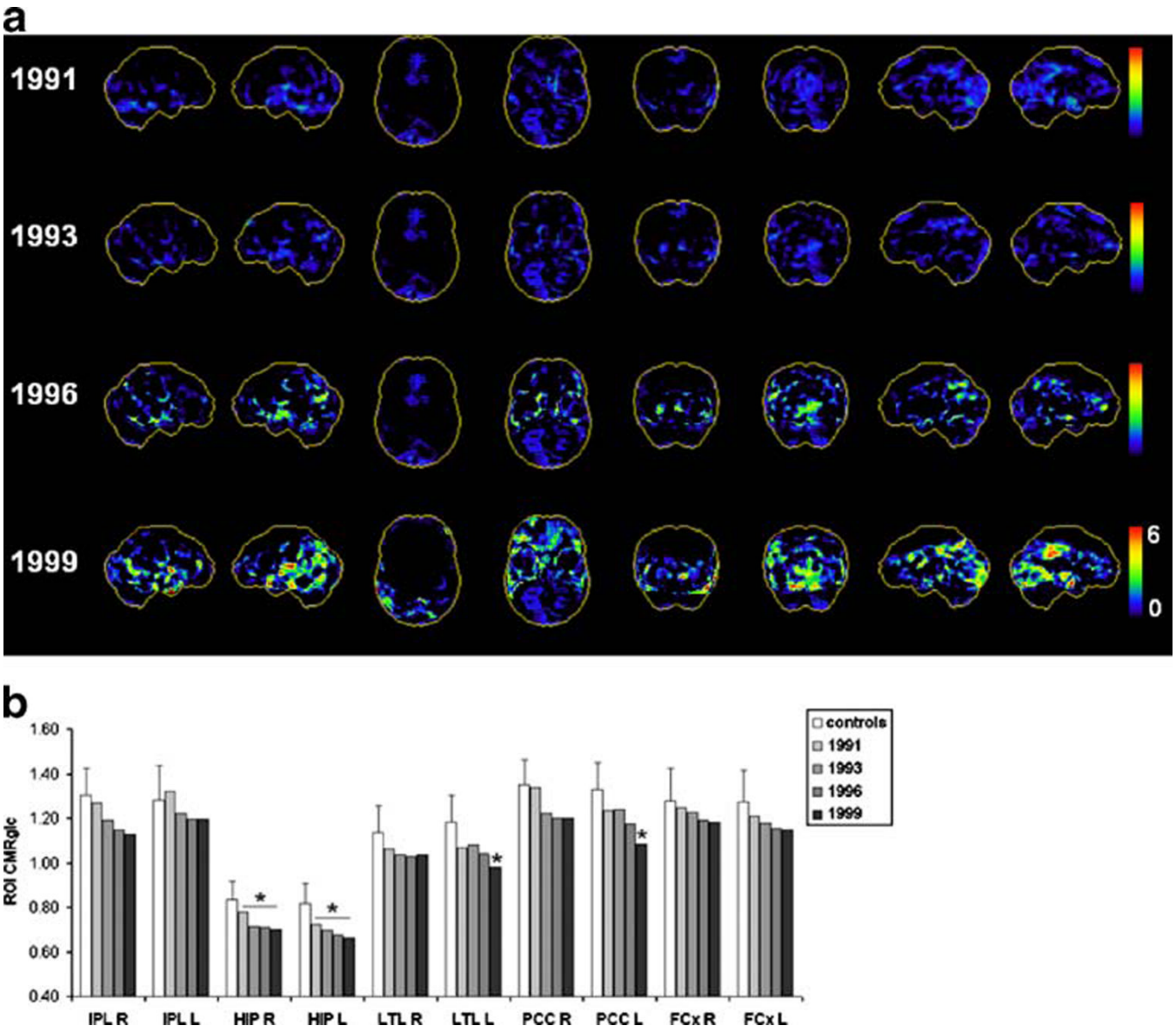

Fig. 1.

Progression of CMRglc abnormalities in patient 1 who declined from normal cognition to MCI and received a postmortem diagnosis of probable AD. **a** 3D-SSP maps and corresponding Z scores reflecting CMRglc reductions in the patient as compared with the normative database are displayed using a color-coded scale ranging from 0 (*black*)to 6(*red*) on the right and left lateral, superior, inferior, anterior, posterior, right and left medial views of a standardized brain template image. **b** Regional CMRglc values at each timepoint are compared to reference control values (white; error bars are standard errors) [25]. *$p \leq 0.05$ vs controls (*IPL* inferior parietal lobe, *HIP* hippocampus, *LTL* lateral temporal lobe, *PCC* posterior cingulate cortex, *FCx* frontal cortex; *L* left, *R* right hemisphere)

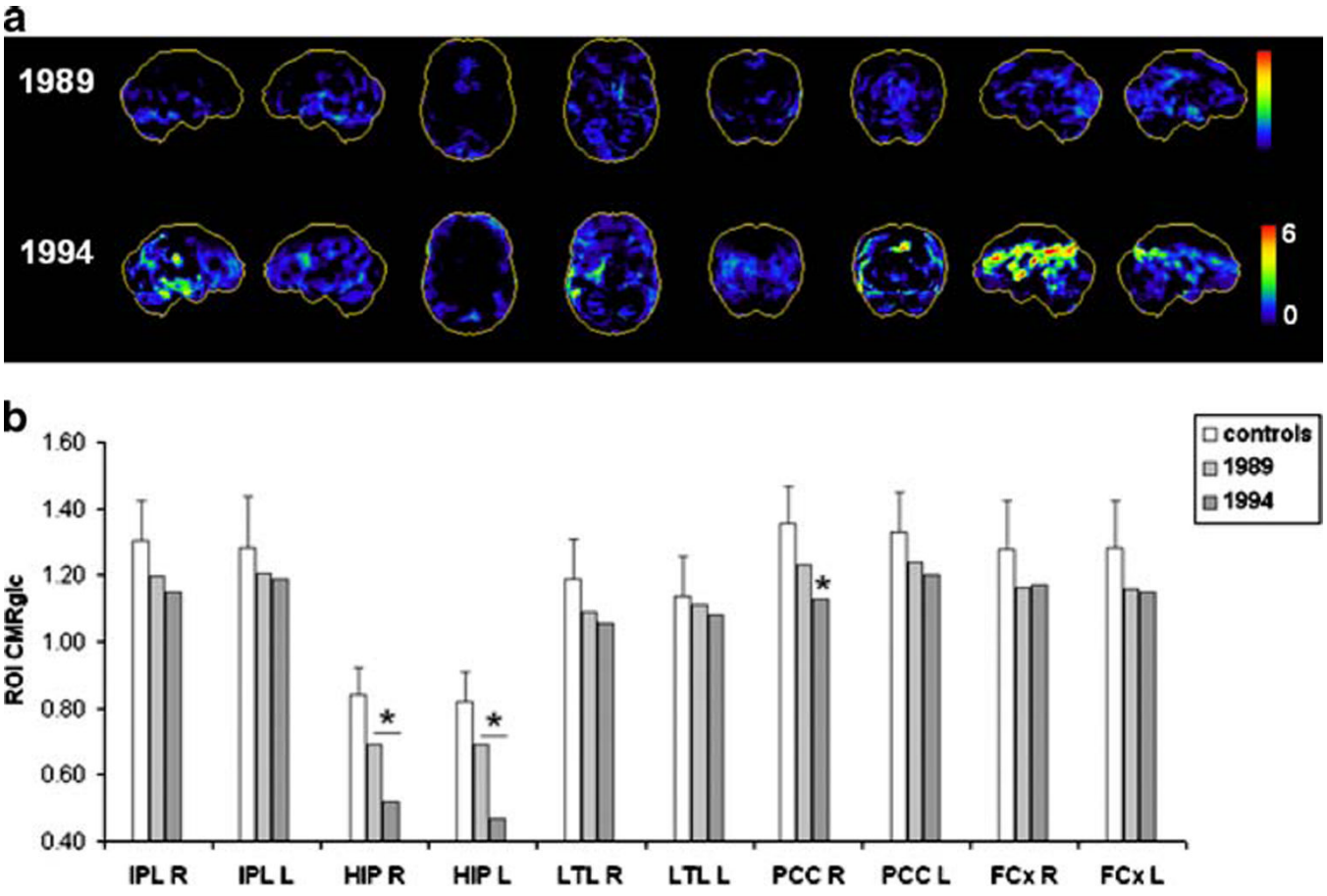

fig. 2.

Progression of CMRglc abnormalities in patient 2 who declined from normal cognition to MCI and received a postmortem diagnosis of Parkinson's disease with additional AD-related pathological lesions. **a, b** *See legend to Fig. 1*

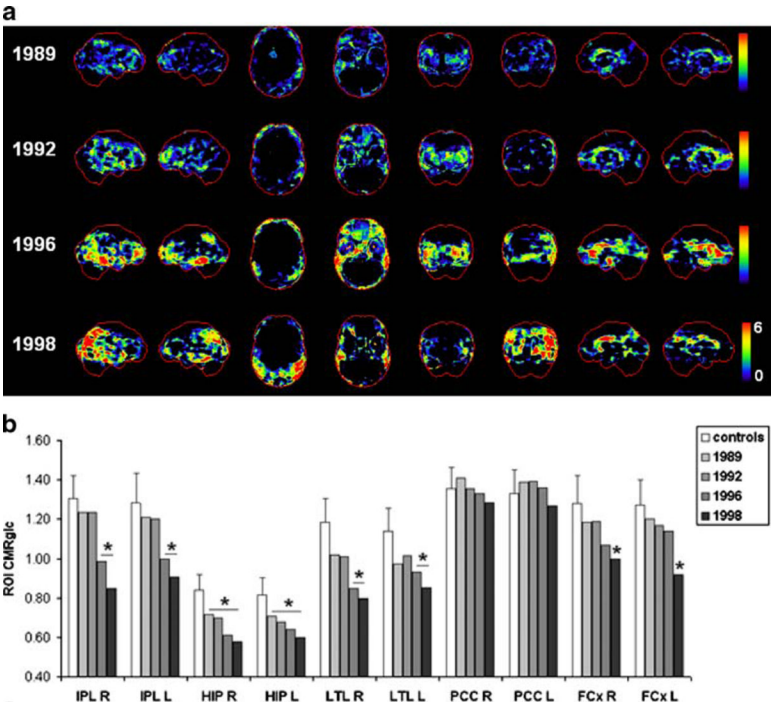

Fig. 3.

Progression of CMRglc abnormalities in patient 3 who declined from normal cognition to DAT and received a postmortem diagnosis of definite AD. **a, b** *See legend to Fig. 1*

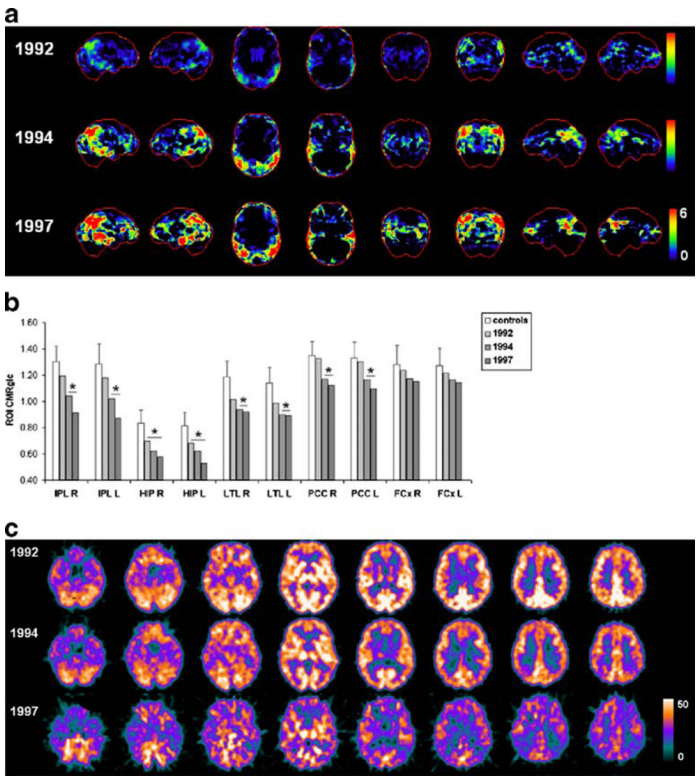

Fig. 4.

Progression of CMRglc abnormalities in patient 4 who declined from normal cognition to DAT and received a postmortem diagnosis of definite AD. **a, b** *See legend to Fig. 1*. **c** Original FDG-PET scans are displayed as transaxial slices 10 mm apart from the bottom (*left*) to the top (*right*) of the brain. CMRglc values are displayed on a color-coded scale ranging from 0 to 50 μmol/ 100 g per minute

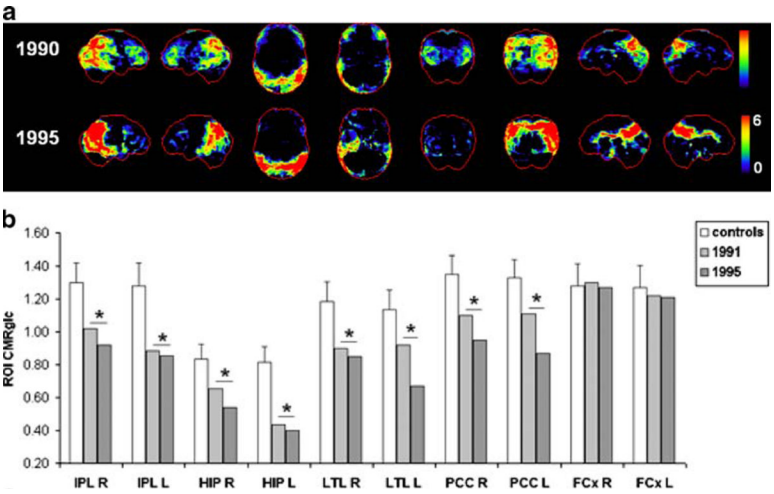

Fig. 5.

Progression of CMRglc abnormalities in patient 5 who progressed from mild to severe DAT in life, and received a postmortem diagnosis of definite AD. **a, b** *See legend to Fig. 1*

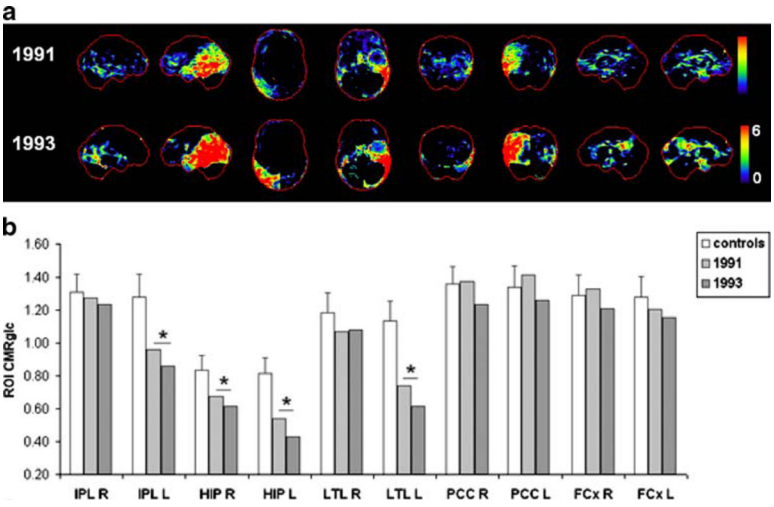

Fig. 6.

Progression of CMRglc abnormalities in patient 6 who progressed from mild DAT to probable vascular dementia in life and received a post-mortem diagnosis of definite AD. **a, b** *See legend to Fig. 1*

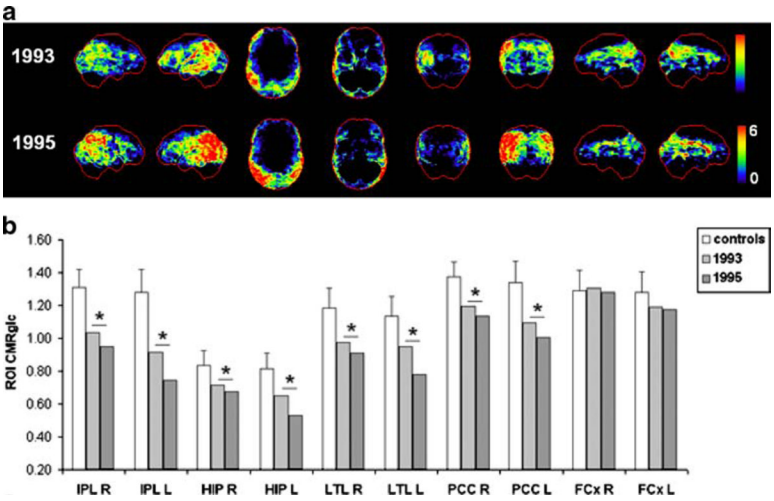

Fig. 7.

Progression of CMRglc abnormalities in patient 7 who progressed from mild to moderate DAT in life and received a post-mortem diagnosis of definite AD. **a, b** *See legend to Fig. 1*

Table 1

Subjects' characteristics

	Patient 1	Patient 2	Patient 3	Patient 4	Patient 5	Patient 6	Patient 7
Age at baseline clinical examination (years)	70	71	69	69	64	69	77
Age at baseline PET (years)	81	80	69	69	66	69	77
Age at death (years)	91	93	85	81	77	79	84
Gender	M	M	F	F	M	F	M
Education (years)	18	16	12	14	12	12	12
ApoE genotype	ε3/ε4	ε3/ε4	ε2/ε4	ε3/ε4	ε3/ε3	ε2/ε4	ε3/ε3
Time from baseline to last examination (years)							
Clinical examination interval	19	14	9	10	12	7	7
PET examination interval	8	5	9	5	5	2	2
Time from last PET to demise (years)	2	8	6	6	6	7	5
GDS score							
Baseline PET	2	2	2	2	6	4	4
Last PET follow-up	3	3	4	5	6	5	5
Clinical diagnosis							
Baseline PET	NL	NL	NL	NL	DAT	DAT	DAT
Last PET follow-up	MCI	MCI	DAT	DAT	DAT	Vascular dementia	DAT
Post-mortem diagnosis	Probable	Parkinson's disease	Definite AD	Definite AD	Definite AD	Definite AD	Definite AD
Other features	AD	Mild AD	Mild subcortical leukoencephalopathy	LBD, congophilic angiopathy	LBD, congophilic angiopathy	Congophilic angiopathy, subcortical leukoencephalopathy	Congophilic angiopathy, subcortical leukoencephalopathy
CERAD	Possible	Possible	Definite	Definite	Definite	Definite	Definite
Braak stage	IV	III	VI	VI	V	VI	V
Neuropsychological measures							
MMSE							
Baseline PET	29	30	30	29	16	27	27
Last PET follow-up	29	27	25	23	2	1	20
Designs							
Baseline PET	10	5	5	7	3	2	2
Last PET follow-up	5	2	2	0	0	1	0
DSST							
Baseline PET	47	41	42	46	0	51	30
Last PET follow-up	29	34	29	40	n.c.	18	n.c.
Object naming							
Baseline PET	60	59	47	39	n.c.	n.c.	n.c.
Last PET follow-up	54	46	42	37			
Paired associates-delayed recall							
Baseline PET	10.5	13.5	6.5	5	5	1	2.5
Last PET follow-up	8	3.5	2	1	n.c.	n.c.	n.c.
Paragraph recall-delayed recall							
Baseline PET	3	6	1	2	0	0	3
Last PET follow-up	3	1	0	0	n.c.	n.c.	n.c.
Visual recognition							
Baseline PET	25	25	18	25	n.c.	n.c.	n.c.
Last PET follow-up	20	17	8	23			

*n.c.*not completed.